

Research Article

# Effect of Polyethylene Glycol Concentration on the Structural and Mechanical Properties of Polysulfone-Based Membranes

Ranti Nur Aprilianti<sup>1,3</sup>, Maulida Rahayu<sup>1,3</sup>, Arie Hardian<sup>2,3</sup>, Anceu Murniati<sup>2,3\*</sup>

<sup>1</sup>Department of Chemistry, Faculty of Sciences and Informatics, Universitas Jenderal Achmad Yani, Cimahi, Indonesia.

<sup>2</sup>Departemen of Master Chemistry, Faculty of Science and Informatics, Universitas Jenderal Achmad Yani, Cimahi, Indonesia

<sup>3</sup>Material and Environmental Development Center of Universitas Jenderal Achmad Yani, Cimahi, Indonesia

\*Correspondence:

anceu.murniati@lecture.unjani.ac.id

## Abstract

Water pollution in Indonesia is a growing concern, necessitating the development of advanced treatment technologies. Membrane-based filtration, a promising approach due to its low energy consumption and ability to preserve material properties, has been explored. Polysulfone (PSf), a commonly used membrane material, is known for its thermal stability, chemical resistance, and mechanical strength. However, its hydrophobic nature limits its filtration performance. To enhance hydrophilicity and porosity, polyethylene glycol (PEG) is introduced as a hydrophilic additive. This study investigated the synthesis of PSf/PEG composite membranes with varying PEG concentrations (0%, 9%, and 14%) using the phase inversion method. Characterization of the membranes revealed that increasing PEG content led to thinner membranes with higher porosity, density, and swelling capacity. While Membrane-A (100% PSf) exhibited the highest tensile strength, Membrane-B (9% PEG) demonstrated the greatest elongation. SEM analysis confirmed that higher PEG concentrations resulted in larger and more numerous pores, forming asymmetric structures suitable for filtration. FTIR analysis verified the successful integration of PEG into the PSf matrix. The findings highlight the potential of PEG-modified PSf membranes for industrial wastewater treatment. The M-C membrane, containing 14% PEG, exhibited the highest swelling degree, indicating improved hydrophilicity and permeability. However, increased PEG content also led to decreased tensile strength. The optimized M-C membrane, with a density of 0.9906 g/cm<sup>3</sup>, a mass of 1.9249 g, and a thickness of 102 μm, meets the requirements for effective water treatment applications. This research contributes to the development of sustainable membrane technologies for environmental management in Indonesia. By addressing the limitations of PSf membranes, PSf/PEG composite membranes offer a promising solution to water pollution challenges in the region.

**Keyword:** Membrane, polysulfone, polyethylene glycol, membrane

## 1. Introduction

Water pollution in Indonesia is of increasing concern, with many industries discharging waste without the treatment process regulated by the Regulation of the Minister of Environment of the Republic of Indonesia Number 5 of 2014 concerning Wastewater Quality Standards [1]. Experts in the

modern chemical industry have developed various technologies to address the decline in water quality. One technology that is widely developed is membrane-based. The main advantage of this membrane technology is that it can prevent material damage caused by high temperatures and low process temperatures, and it requires a fairly low amount of

energy. A membrane is a semipermeable barrier that can pass certain parts but retain other parts in controlling the permeation of certain components [2]. Based on research [3] membranes can be used in waste treatment because they exhibit effective activities in supporting the degradation of phenol-contaminated waste. Membranes are divided into two types based on morphology: asymmetric and symmetric. Asymmetric membranes consist of a thin, tight layer with a 0.1–0.5  $\mu\text{m}$  thickness and a large porous support layer with a 50–150  $\mu\text{m}$  thickness. Meanwhile, symmetric membranes have pores with a 10–200  $\mu\text{m}$  thickness and a homogeneous pore structure throughout the membrane [4].

PSf is a thermoplastic polymer commonly used as a membrane base material for various industrial applications, especially in ultrafiltration processes [5]. The structure of PSf having repeating units  $[\text{OC}_6\text{H}_4\text{OC}_6\text{H}_4\text{SO}_2\text{C}_6\text{H}_4]_n$  exhibits excellent properties, such as high thermal stability (150–170°C), consistent chemical stability across the pH range, mechanical strength that includes fracture toughness, flexibility, and torsion, and optimal processability [6]. However, the hydrophobicity of PSf can reduce the membrane's performance as a filter. Therefore, blending with materials such as PEG is necessary to improve the stability of membrane performance, which in turn can improve the hydrophilic nature of the membrane as well as its water flux value [7]. Polymer membranes with high water permeability are often combined with additives, such as polyvinyl pyrrolidone (PVP) and PEG. PEG has hydrophilic properties that improve membrane performance and the potential to increase the porosity and water permeability of the membrane [8].

In this study, a composite of PSf with PEG will be prepared to form a membrane (PSf/PEG) that is expected to have optimal performance. The characteristics of the PSf/PEG membrane will be tested using various physical parameters, including the degree of swelling, to determine the ability of the membrane to absorb certain liquids or materials, as well as to understand the changes in membrane volume and structure that occur as a

result of the absorption process [9]. Other tests include membrane thickness characterization to determine the permeation rate, tensile strength tests performed to obtain data related to deformation (strain) and applied force (stress) over a range of minimum to maximum conditions to evaluate mechanical properties, and SEM image to observe the surface and transverse structure of the membrane. Our previous research has focused on the preparation of polymer-based membrane and immobilization systems of polyphenol oxidase enzymes, as well as their application in industrial waste treatment [10-12].

## 2. Materials and methods

### 2.1. Material

All chemicals used were selected with high analytical quality and obtained from Sigma-Aldrich, including Polysulfone  $[\text{OC}_6\text{H}_4\text{OC}_6\text{H}_4\text{SO}_2\text{C}_6\text{H}_4]_n$  1700 NT LCD from Solvay, N-Dimethylformamide ( $\text{C}_3\text{H}_7\text{NO}$ ), Polyethylene Glycol ( $\text{H}(\text{O}-\text{CH}_2\text{CH}_2)_n\text{OH}$ ), distilled water ( $\text{H}_2\text{O}$ ) and acetone ( $\text{C}_3\text{H}_6\text{O}$ ).

### 2.2. Laboratory Equipment and Instrumentation

The equipment used includes laboratory glassware, membrane printer, membrane printing apparatus and digital millimeter, instrumentation equipment: scanning electron microscopy (SEM) series JEOL JSM-6510LA and tensile strength brand Shimadzu AGx 690, FTIR brand Shimadzu.

### 2.3. Preparation of Polysulfone/ Polyethylene Glycol Solution

#### *Preparation of Solution A: PSf without PEG*

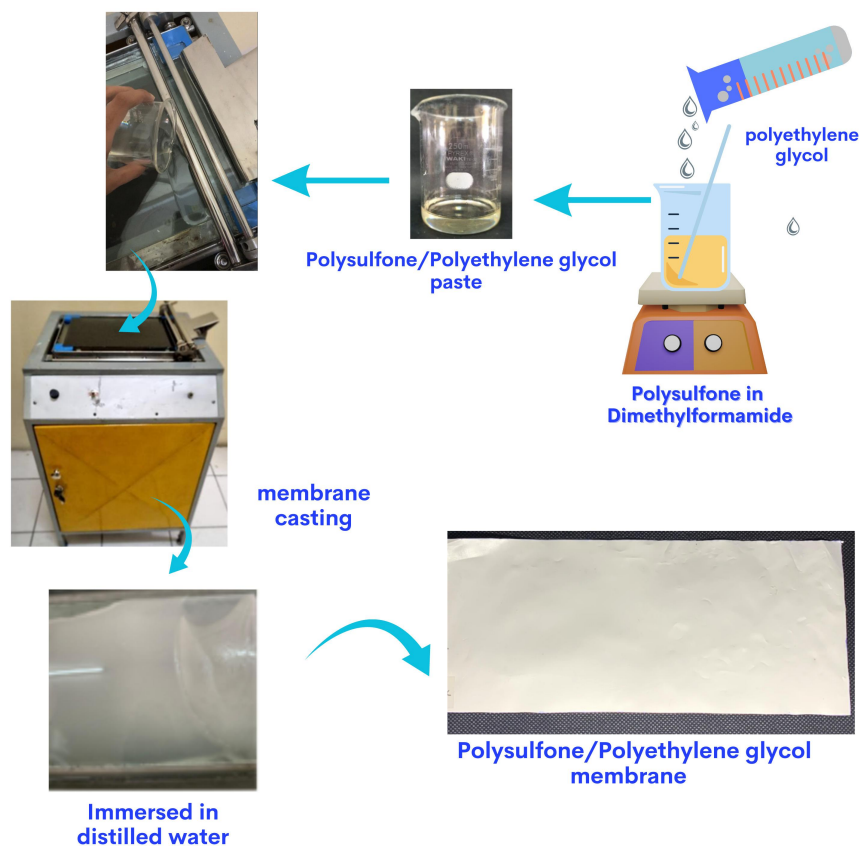
Solution A was prepared by dissolving polysulfone (PSf) in 30 mL of dimethylformamide (DMF) at 60°C. The mixture was stirred using a magnetic stirrer for approximately 2 hours until a homogeneous solution was achieved. The resulting solution was a clear, thick paste.

#### *Preparation of Solution B: PSf with PEG*

Solution B, a mixture of 91% PSf and 9% polyethylene glycol (PEG), was prepared by first dissolving the PSf in 30 mL of DMF. Subsequently, 3 mL of PEG was added to the mixture. The homogenization process was carried out using a magnetic stirrer for approximately 2 hours until a clear yellow thick solution (paste) was formed.

**Table 1.** Composition of the PSf/PEG solutions.

The membrane codes	PSf and PEG	PSf (%)	PEG (%)
M-A membrane	PSf without PEG	100	0
M-B membrane	PSf with PEG	91	9
M-C membrane	PSf with PEG	86	14

**Figure 1.** The membrane synthesis stages: preparation of PSf/PEG solutions in Dimethylformamide (DMF), formation of paste, and PSf/PEG membrane.**Preparation of Solution C: PSf with PEG**

Solution C, a mixture of 86% PSf and 14% PEG, was prepared by first dissolving the PSf in 30 mL of DMF. Subsequently, 5 mL of PEG was added to the mixture. The homogenization process was carried out using a magnetic stirrer for approximately 2 hours until a clear yellow thick solution (paste) similar to Solution B was formed.

**2.4. Preparation of Polysulfone/ Polyethylene Glycol****Solution**

Solutions A, B, and C were cast by slowly pouring them onto a glass plate using a membrane printer. The glass plate was positioned to ensure the solution spread evenly in a thin layer across its surface. Care was taken during casting to achieve the desired layer thickness. Subsequently, the mold was immersed

in room temperature distilled water for 15 minutes to separate the membrane layer. The formed membrane was then dried in an oven at 30°C for 10 minutes until fully dry.

## 2.5. Membrane Characterization

### Swelling Degree

The membrane was dried for 5 hours at 40 °C in an oven then weighed dry weight ( $W_0$ ). Then the membrane was soaked in distilled water for 24 hours and weighed to determine the wet weight ( $W_1$ ) [8] (Equation=1):

$$\text{Degree of Swelling} = \frac{(W_1 - W_0)}{W_0} \times 100\%$$

(Equation=1)

### Membrane thickness measurement

The membrane was measured using a digital millimeter on four different sides, then the measurement results were summed up, and the average was taken as the result of the membrane thickness [4].

### Membrane Mass Measurement

The mass scale was first measured without the membrane, and then the membrane was placed on the analytical scale

### ASTM D-638-02 standard tensile strength test

The indicator on the tensile strength testing machine is made zero first, then the membrane is attached to the tool by clamping it right on the test specimen holder then the program on the computer is set to run the tensile test tool.

### SEM (Scanning Electron Microscopy) test

To determine the thickness and pores of the membrane The membrane samples were dried and then immersed in liquid nitrogen for four hours. Using tweezers, the samples were removed and broken at both ends. Subsequently, membrane pieces measuring 0.5×0.5 cm were coated with pure gold. The cross-sectional surface of the membrane was used for morphology observation at a voltage of 15 kV. SEM analysis was performed at various magnifications, including 150×, 500×, 1,000×, and up to 10,000×, to examine the surface and cross-sectional morphology of each membrane. The SEM conditions were set with a working distance and an accelerating voltage of 5 kV to produce high-quality images. Additionally, membrane thickness was measured using a

digital micrometer to compare the SEM observations with actual thickness measurements.

### The FTIR (Fourier Transform Infrared) analysis of the PSf/PEG composite

The FTIR analysis of the PSf/PEG composite begins with preparing the membrane by cutting it into small, thin pieces to ensure optimal infrared light transmission. The spectrum is then recorded over a wavenumber range of 4000  $\text{cm}^{-1}$  to 400  $\text{cm}^{-1}$ , averaging multiple scans to improve signal quality. Key absorption peaks corresponding to the functional groups of polysulfone (PSf) and polyethylene glycol (PEG) are identified. These peaks confirm the successful integration of PEG into the polysulfone matrix, verifying the formation of the composite. Finally, the obtained spectra are analyzed and compared with reference data, and a detailed report is generated, highlighting the characteristic peaks and functional groups present in the membrane[7].

## 2.6. Membrane Performance Test

The dried PSf membrane, shaped into a flat sheet, was positioned within a tubular membrane housing. The membrane had a surface area of 0.0298  $\text{m}^2$  and a thickness of 68  $\mu\text{m}$ . Its performance was assessed using a continuous cross-flow filtration system with 12 liters of synthetic wastewater. Permeate was collected after each liter, and testing was conducted over 10 cycles to evaluate the membrane's performance in terms of flow rate, flux, and permeability. The flow rate (Q) was calculated using the following equation 2):

$$Q = \frac{V}{t} \quad (\text{Equation}=2)$$

where (Q) represents the flow rate (L/h), V is the permeate volume (L), and t is the time (h) [4].

Flux (J) was determined by the equation 3 :

$$J = \frac{V}{A.t} \quad (\text{Equation}=3)$$

where J is the flux ( $\text{L/h}\cdot\text{m}^2$ ), V is the permeate volume (L), t is the time (h), and A is the membrane surface area ( $\text{m}^2$ ) [4].

The membrane permeability was calculated using the equation 4):

$$\text{Permeability } y = \frac{\text{Flux}}{\Delta P} \quad (\text{Equation}=4)$$

where permeability is derived from the measured flux and the transmembrane pressure [4]. Phenol rejection was also evaluated to determine the efficiency of the PSf membrane in removing phenol. The percentage rejection (%R) was defined by the equation 5:

$$\%R = 1 - \frac{C_p}{C_f} \times 100\% \quad (\text{Equation} = 5)$$

where  $C_p$  refers to the permeate concentration (ppm) and  $C_f$  is the feed concentration (ppm) [4].

### 3. Results and discussion

#### 3.1. Preparation of Polyethylene Glycol modified Polysulfone Membrane

Preparation of PSf membranes involved modifying them with additives, specifically PEG. In this study, membranes included PSf without PEG (M-A), PSf with 9% PEG (M-B), and PSf with 14% PEG (M-C). Figure 2 shows there is no visible difference among the three PEG concentration variations to the naked eye. However, differences in concentration indicate that higher levels of PEG result in thinner membranes. Table 2 outlines the physical characteristics of these variations.

The addition of PEG aims to increase pore size and membrane permeability, as well as enhance thermal and hydrophilic properties, thus reducing fouling on hydrophilic membranes

[13]. The membrane casting process utilized a membrane printer consisting of a glass plate and an iron rod. Membranes were cast at a molding speed of 100 rpm to ensure uniformity. Subsequently, membranes were immersed in a coagulation bath containing nonsolvent compounds during the phase inversion process [14].

#### 3.2. Membrane characterization

##### Membrane density

The addition of PEG can enhance the density of PSf membranes by acting as a matrix filler, filling the spaces between polymer molecules and thereby increasing membrane density. Higher concentrations of PEG can lead to membranes with smaller and more uniform pores, potentially impacting membrane density [15]. Research findings show that M-C demonstrates superior mechanical strength compared to other membranes, as shown in Table 2. Table 2 show that membranes without PEG modifications are lighter than those with PEG additions, with higher concentrations of PEG correlating to greater membrane weights. Thus, the sequence of membrane weight comparison is as follows: M-A < M-B < M-C.

##### Membrane thickness

The membrane thickness is determined using a digital micrometer at five different points: top, bottom, right, left, and center, detailed in Table 2. The thickness is influenced by the PSf polymer concentration; higher concentrations result in thicker membranes. The casting process also affects thickness, especially if the dope solution is unevenly applied on the glass plate [16].

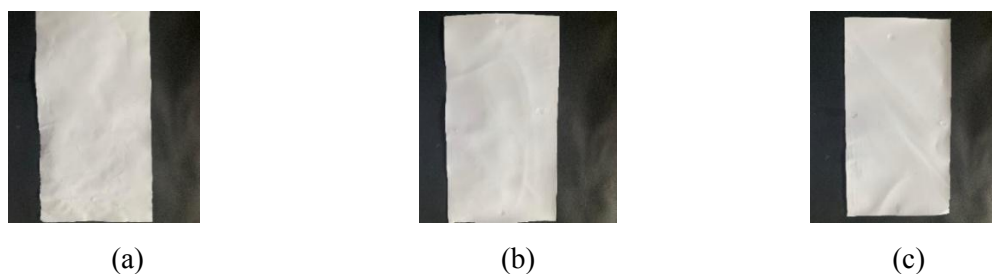


**Figure 2.** The physical appearance of membranes with 3 composition variations: (a). Membrane-A (M-A): PSf 100% without PEG, (b). Membrane-B (M-B): PSf 91% with 9% PEG, (c). Membrane-C (M-C): PSf 86% with 14% PEG.



**Table 2.** Characterization of membranes, including measurements of density, mass, thickness, and swelling

The membrane codes	Mass (g)	Thickness ( $\mu\text{m}$ )	Density ( $\text{g}/\text{cm}^3$ )	Swelling (%)
Membrane-A (M-A)	$0.7730 \pm 0.067$	$144 \pm 0.075$	$0.355 \pm 0.196$	126.18
Membrane-B (M-B)	$1.5770 \pm 0.303$	$113 \pm 0.066$	$0.948 \pm 0.642$	216.92
Membrane-C (M-C)	$1.9249 \pm 0.303$	$102 \pm 0.072$	$1.325 \pm 0.660$	220.12

The measurements of the three membranes are: M-A at  $144 \pm 0.075 \mu\text{m}$ , M-B at  $113 \pm 0.066 \mu\text{m}$ , and M-C at  $102 \pm 0.072 \mu\text{m}$ . According to [4], ultrafiltration membranes are typically classified with a maximum thickness of about  $150 \mu\text{m}$ , placing all three membranes within this category, as confirmed by this study's results.

#### Degree of membrane swelling

Testing the swelling degree of the membrane helps predict how much a specific solvent or substance can diffuse into it. Swelling can also indicate the presence of voids between polymer bonds, which can impact mechanical properties; smaller voids generally imply better mechanical strength [17]. The swelling test results correlate with the concentration of

added PEG: higher concentrations lead to increased swelling. This is because higher PEG concentrations create more space between molecules and larger pores in the membrane, facilitating easier water diffusion and greater expansion capability [18]. In this study, the resulting swelling can be observed in Table 2. Swelling degree is determined by the gravimetric method by calculating the difference between dry mass and wet mass. Membranes whose water absorption degree is more than 50% can be used for filtration [19]. The literature confirms the findings presented in Table 2. The swelling degrees are 126.18%, 216.92%, and 220.12%, indicating that the PSf/PEG membranes are suitable for use as filtration membranes.

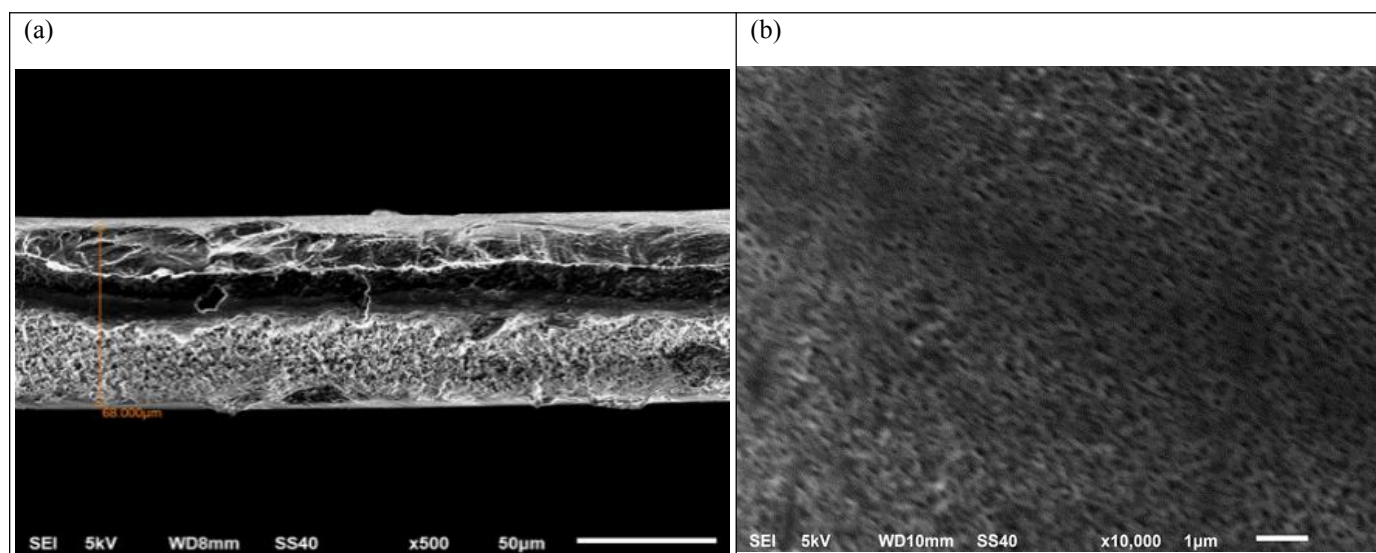


**Figure 3.** SEM images of M-A membrane made from PSf 100% without PEG, showing (a) cross-sectional morphology and (b) surface morphology.

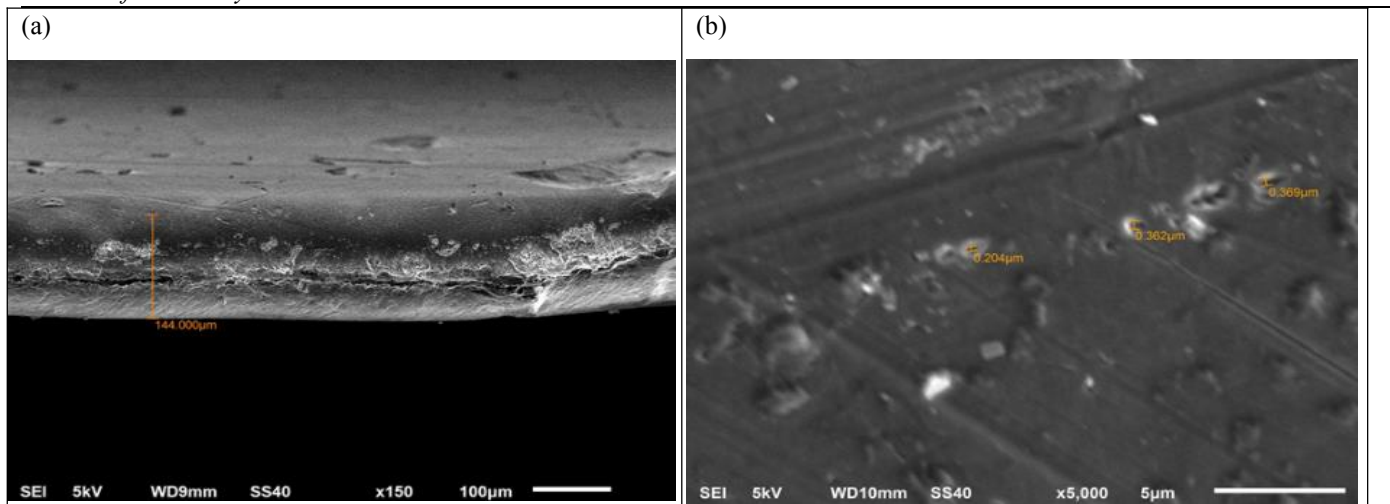


**Figure 4.** shows SEM images of M-B membrane, PSf 91% with 9% PEG, depicting (a) cross-sectional and (b) surface morphology.

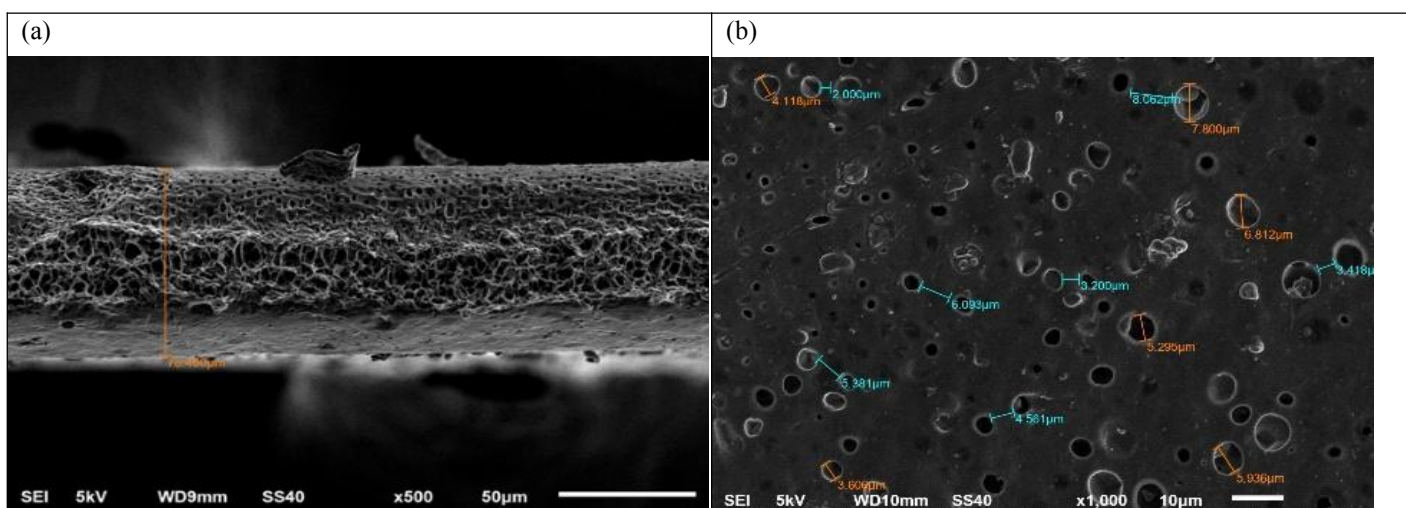


**Figure 5.** SEM images of M-C membrane, PSf 86% with 14% PEG, showing (a) cross-sectional and (b) surface morphology.

### 3.3. SEM images of PSf membranes without and with PEG

The SEM images in Figures 3, 4, and 5 offer valuable insights into the structural and morphological properties of membranes M-A, M-B, and M-C. SEM imaging parameters included a working distance and an accelerating voltage of 5 kV. At 150x magnification (Figure 3a), M-A membrane (without PEG) exhibits a thickness of 144  $\mu\text{m}$ , consistent with the digital micrometer measurement ( $144 \pm 0.075 \mu\text{m}$ ) in Table 2. In Figure 3b, at 5000x magnification, M-A membrane morphology shows a surface with small pores ranging from 0.204 to 0.369  $\mu\text{m}$ , spaced apart significantly, indicating low pore density. This SEM analysis confirms that M-A membrane (PSf without PEG) qualifies as an ultrafiltration membrane,

meeting criteria typically set for ultrafiltration membranes with thicknesses around 150  $\mu\text{m}$  and pore sizes ranging from 0.001 to 2.00  $\mu\text{m}$ . In Figure 4, SEM analysis of the M-B membrane at 500 $\times$  for cross-sectional profiles and 10,000 $\times$  for morphological profiles revealed the presence of surface cavities or pores.

This is in stark contrast to the M-A membrane (PSf without PEG), illustrating that the addition of 9% PEG effectively induces pore formation as a porogen additive. The incorporation of PEG results in a thinner M-B membrane. PEG serves as a pore-forming agent, promoting nucleation when the printed membrane is immersed in the coagulation bath [20]. However, the observed pores are small due to the low

concentration of PEG used. Despite its reduced thickness of 68.00  $\mu\text{m}$  compared to Table-2's  $113 \pm 0.066 \mu\text{m}$ , it still classifies as an ultrafiltration membrane according to Mulder's classification.

SEM images of M-C membrane, composed of 86% PSf and 14% PEG, depict (Figure 5a at 500 $\times$  magnification) cross-sectional and (Figure 5b at 1,000 $\times$  magnification) surface morphology. Figure 5a shows the SEM analysis of the M-C membrane, revealing clearly visible pores in both cross-sectional and surface views, highlighting the effectiveness of PEG as a porogen additive. The formation mechanism of the fingerlike pore structure in the membrane is governed by kinetic factors associated with mass transfer during immersion in the coagulation bath, involving interactions between the solvent (DMF) and non-solvent (water). Rapid liquid-liquid demixing occurs upon direct contact of PSf with water, triggering immediate pore formation [21].

The hydrophilic properties of PEG expedite the exchange of solvent and non-solvent, thereby promoting an increase in cavities within the membrane's structural layer. However, the influence of PEG on pore size can be variable, as observed in previous research [13], where its application in sulfonated polyphenylene sulfone (sPPSU) membranes led to a reduction in pore size. Consequently, the effect of PEG on membrane properties is contingent upon the specific characteristics of the polymers comprising the membrane.

### 3.4 Physical properties characterization of Polysulfone membranes with and without Polyethylene Glycol

To determine the mechanical properties of the membrane, tensile strength and percentage elongation tests were conducted. The tensile strength value indicates the strength of the membrane when given a certain tensile strength, and the percentage of elongation indicates the elasticity of the membrane when stretched to its maximum [22].

The results of this test are shown in Table 3. To assess the impact of PSf and PEG concentrations on membrane strength, the mechanical properties of PSf/PEG membranes were evaluated using tensile strength and elongation tests. The

results in Table 3 reveal that increasing PEG concentration decreases membrane tensile strength. This decline is attributed to the reduced PSf concentration, as higher polymer concentrations typically enhance tensile strength. Specifically, the M-A membrane exhibits the

highest tensile strength at 5.68 N/mm<sup>2</sup> followed by membrane B at 3.74 N/mm<sup>2</sup>, and membrane C at 2.57 N/mm<sup>2</sup>

In contrast, elongation results in Table 3 show variations compared to tensile strength. Membrane B demonstrates increased elongation, contrary to the tensile strength trend. This phenomenon is influenced by PEG, a highly hydrophilic polymer capable of interacting with other membrane components to enhance elongation properties. Elongation shows how long the membrane can be stretched before breaking [23]. It occurs in membrane B, but PEG can also reduce elongation if the concentration of PEG is too high due to the interaction of water with the membrane becomes stronger due to the increasing number of hydrophilic groups per unit surface area of the membrane so that the resulting mechanical strength is reduced [24].

**Table 3.** The tensile strength and elongation properties of PSf membranes without and with PEG

Membrane composition	The membrane codes	Tensile Strength (N/mm <sup>2</sup> )	Elongation (%)
PSf membranes without PEG	M-A membrane	5.68	56.67
PSf membranes with PEG	M-B membrane	3.74	80.00
PSf membranes with PEG	M-C membrane	2.57	35.00

The findings of this study, particularly regarding the increase in porosity and permeability with higher PEG concentrations in PSf/PEG membranes, are consistent with previous research on membrane modification.



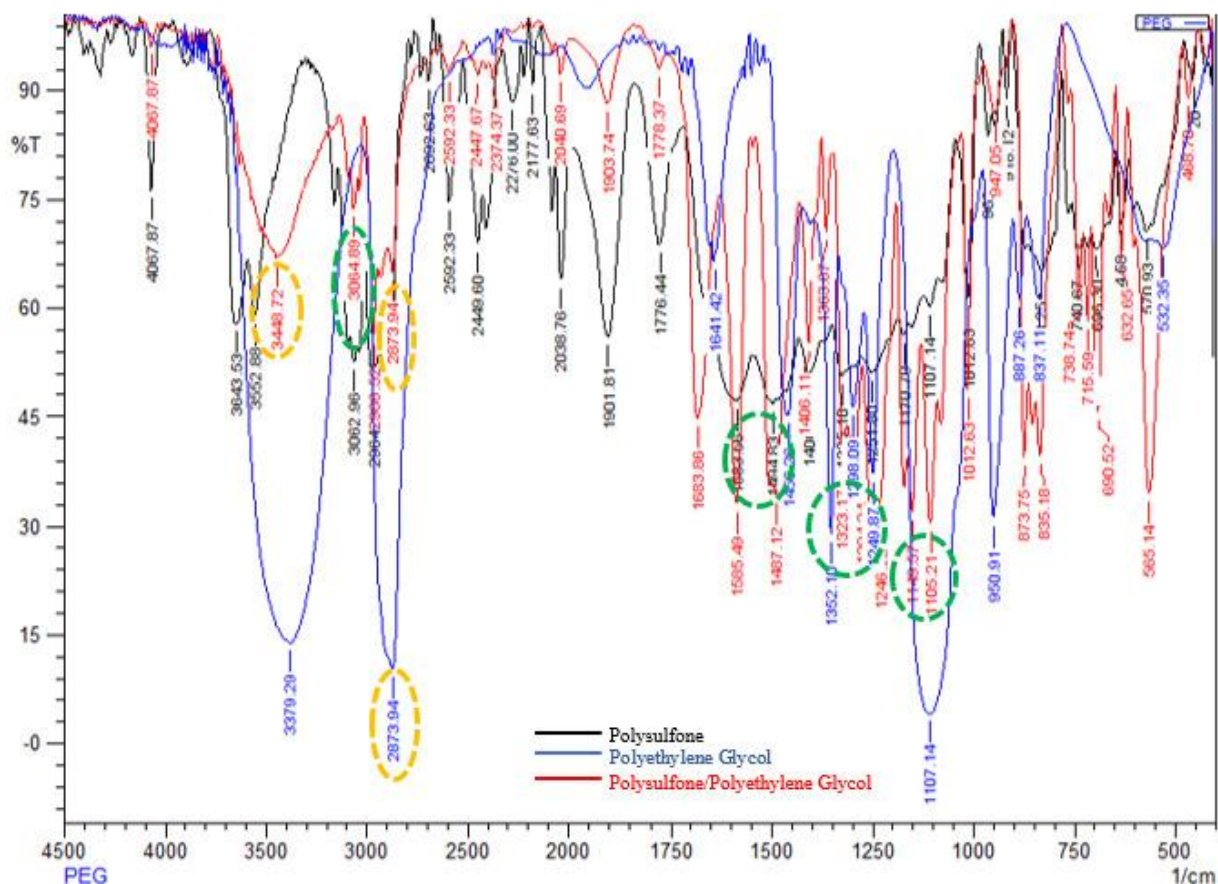


**Figure 6:** FTIR spectrum of PSf/PEG membrane, showing characteristic absorption peaks corresponding to the Polysulfone (PSf) and Polyethylene glycol (PEG) components.

Similar studies, such as those conducted by [25] have demonstrated that the incorporation of hydrophilic additives like PEG significantly enhances water absorption capacity and reduces membrane fouling by improving the hydrophilicity of the membrane.

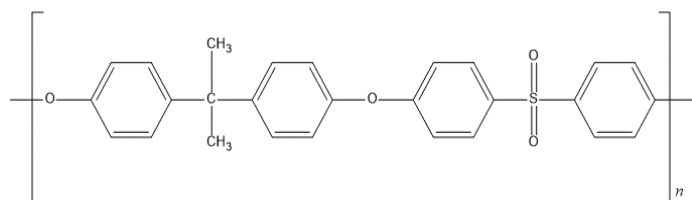


**Figure 7.** Chemical structure of Polysulfone (PSf), illustrating the repeating aryl-sulfone units that contribute to its thermal stability, mechanical strength, and chemical resistance.

However, our study offers a more comprehensive analysis of the balance between permeability and mechanical strength. We found that although higher PEG concentrations increase porosity and water flux, they also result in a decrease in tensile strength. This finding contrasts with studies that primarily focus on permeability improvements without addressing the mechanical trade-offs. Thus, our results provide a more nuanced understanding of the effects of PEG concentration on both the structural and functional performance of PSf-based membranes.

The structure of PSf/PEG copolymers is influenced by the ratio of PSf and PEG segments, their sequence arrangement, and the chain length of each segment. A higher proportion of PEG

segments imparts flexibility, while a higher proportion of PSf segments confers rigidity due to their aromatic structure.

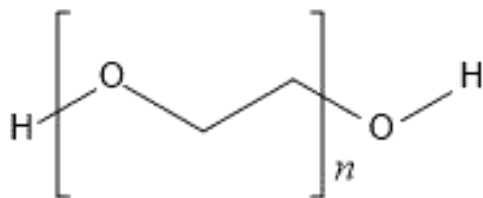


**Figure 8.** Chemical structure of Polyethylene Glycol (PEG), showing the repeating ethylene oxide units that provide hydrophilicity and flexibility to the polymer chain.

The arrangement of segments, whether random, alternating, or in blocks, significantly affects properties like phase behavior and mechanical characteristics. Moreover, longer chains of both PSf and PEG can lead to increased viscosity and altered phase transitions.

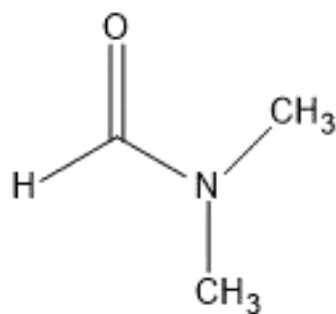


**Figure 9.** Chemical structure of Dimethylformamide (DMF), a polar aprotic solvent commonly used in polymer synthesis and membrane fabrication processes.

### 3.5 FTIR Analysis for Confirmation of Polysulfone /Polyethylene Glycol Composite Formation

FTIR analysis confirms the successful integration of PEG into the PSf matrix by identifying characteristic absorption peaks corresponding to the functional groups of both components. The presence of the hydroxyl (OH) group from PEG is evident at around  $3448.72\text{ cm}^{-1}$ , indicating its hydrophilic nature and ability to interact with water. Additionally, the C-H stretching vibrations of the aromatic rings in PSf are detected at  $3064\text{ cm}^{-1}$ , highlighting the aromatic structure of PSf. The conjugated

C=C bond from the aromatic rings shows absorption in the range of  $1583\text{-}1498\text{ cm}^{-1}$ , further confirming the presence of aromatic components in the composite.

Furthermore, the aliphatic C-H stretching vibrations, mainly from the methylene groups, appear below  $3000\text{ cm}^{-1}$ , with a peak around  $2873\text{ cm}^{-1}$ . This suggests the incorporation of PEG or PSf into the composite. The sulfonic O=S=O group characteristic of PSf is identified by strong absorption between  $1294\text{-}1323\text{ cm}^{-1}$  for asymmetric stretching, with bending vibrations detected at  $1149\text{ cm}^{-1}$  (asymmetric) and  $1105\text{ cm}^{-1}$  (symmetric). These spectral features confirm the coexistence of PSf/PEG within the composite, verifying the successful formation of the PSf/PEG membrane. The presence of a strong hydrogen bonding interaction between the hydroxyl (OH) groups of PEG and the sulfonyl ( $\text{SO}_2$ ) groups of PSf was evident by the significant shift of the OH stretching vibration to a lower wavenumber, approximately  $3448.72\text{ cm}^{-1}$ . This shift indicates the formation of hydrogen bonds, enhancing the hydrophilicity of the composite. Additionally, van der Waals interactions and the heterogeneous chemical environment contributed to the overall properties of the composite. These interactions had a profound impact on the composite's properties, including improved hydrophilicity, mechanical strength, and compatibility between the two polymers. Consequently, the PSf/PEG composite exhibits promising potential for applications in membrane filtration and biomedical devices [26].

While the primary focus of this study was on improving the physical and mechanical properties of the PSf/PEG membranes, such as permeability, porosity, and mechanical strength, toxicity assessment was not conducted. However, previous studies have highlighted the importance of evaluating membrane toxicity, particularly for applications in water filtration. For instance, [27] demonstrated that the incorporation of hydrophilic additives like PEG and chitosan into PSf membranes can improve hydrophilicity and permeability, potentially reducing the membrane's toxicity.

Future studies should include comprehensive toxicity assessments, such as leaching tests to evaluate the release of chemical components, and cytotoxicity and ecotoxicity tests to assess environmental and human health impacts. These evaluations are crucial to ensure that the developed membranes are both effective and environmentally safe for long-term use

### 3.6 Membrane Performance Test

Based on the results obtained from the application of the PSf membrane for phenol removal using a cross-flow filtration system at a pressure of 2 bar, the membrane performance was evaluated in terms of flow rate, flux, and permeability as presented in table 4. :

**Table 4.** Results of Flow Rate, Flux, and Permeability Tests of Polysulfone-PEG Membrane.

Filtration of Artificial Wastewater Using Polysulfone-PEG Membrane (M-C)					
t (s)	t (h)	V (L)	Flow Rate (L/h)	Flux (L/h·m <sup>2</sup> )	Permeability (L/h·m <sup>2</sup> ·bar)
53	0,0147	1	67,92	2279,35	1139,67
61	0,0169	1	59,02	1980,42	990,21
65	0,0181	1	55,38	1858,54	929,27
64	0,0178	1	56,25	1887,58	943,79
63	0,0175	1	57,14	1917,55	958,77
66	0,0183	1	54,55	1830,38	915,19
63	0,0175	1	57,14	1917,55	958,77
62	0,0172	1	58,06	1948,47	974,24
63	0,0175	1	57,14	1917,55	958,77
67	0,0186	1	53,73	1803,07	901,53
Rata-rata			57,63	1934,05	967,02

The flow rate is one of the key factors influencing flux, as a higher flow rate increases the volume of water passing through the membrane, thereby enhancing flux, this occurs because more particles on the membrane surface can be moved by the feed stream [28]. Flux measurement is a critical parameter used to evaluate membrane performance in processing feed volumes. The flux results were unstable due to variations in flow rate. However, a significant decline in flux was observed after the 10th cycle, attributed to fouling or clogging during filtration, which is a common challenge in membrane technology.

Membrane permeability is determined by factors such as pore size, porosity, thickness, and membrane structure. The average permeability of the membrane was 967.02 L/h·m<sup>2</sup>·bar, which, according to [29] falls within the typical range for ultrafiltration membranes ( $\pm 1000$  L/m<sup>2</sup>·h·bar). Thus, the obtained permeability values classify the membrane as an ultrafiltration membrane.

## 4. Conclusion

The findings of this study demonstrate that the addition of polyethylene glycol (PEG) to polysulfone (PSf)-based membranes significantly affects their physical and mechanical properties. The membrane without PEG (M-A) exhibited lower thickness, tensile strength, and swelling degree compared to membranes containing PEG. As PEG concentration increased, the membrane's porosity and water absorption capacity also increased, as indicated by the higher swelling degree in M-B (9% PEG) and M-C (14% PEG) membranes. However, tensile strength decreased with higher PEG content. M-C showed the highest porosity but the lowest tensile strength. SEM analysis confirmed that increased PEG concentration led to larger pores and a more asymmetric membrane structure. Overall, PSf/PEG membranes demonstrate promising potential for filtration applications, particularly in processes requiring hydrophobic membranes with high porosity.

### Authors Contribution

Anceu Murniati (AM) Conceptualization, Methodology, Supervision, Manuscript Review, and Editing; Ranti Nur Aprilianti (RNA) Data Analysis, Manuscript Drafting; Maulida Rahayu (MR) Data Analysis; Arie Hardian (AH) Supervision, Manuscript Review and Editing.

### Conflicts of Interest

There is no conflict of interest between the authors.

### Acknowledgment

We gratefully acknowledge the Ministry of Research, Technology, and Higher Education of the Republic of Indonesia for funding this research through the Master's Thesis Research Scheme (PTM): DRTPM-LLDIKTI

We also extend our appreciation to the Ministry of Education and Culture for their support through the Matching Fund (192/E1/KS.06.02/2022 and 06/PKS/UNJANI/VII/2022), as well as to LPPM UNJANI for providing competitive research funding under grant number 131/UNJANI/V/2024 for the AM Research Group.

#### **Data Availability statement**

The data presented in this study are available on request from the corresponding author.

**Funding:** The Ministry of Education and Culture's Matching Fund support (192/E1/KS.06.02/2022 and 06/PKS/UNJANI/VII/2022) and competitive research funding from LPPM UNJANI under grant number 131/UNJANI/V/2024 for the AM Research Group.

#### **REFERENCES**

1. Balthasar Kambuaya, Regulation of the Minister of Environment of the Republic of Indonesia No. 5 of 2014 concerning Wastewater Quality Standards., (2014). <https://doi:0.1177/003231870005200207>
2. Othman. N. H, Alias. N. H, Fuzil. N. S, Marpani. F, Shahrudin. M. Z, Chew. C. M, K. M. David Ng, Lau. W.J, Ismail. A. F. (2022). A review on the use of membrane technology systems in developing countries, *Membranes*, 12, 30 <https://doi:10.3390/membranes12010030>
3. Murniati. A, Buchari. B, Gandasasmita S, Nurachman. Z, Hardian. A, and Triani. D. (2021). Immobilization of Crude Polyphenol Oxidase Extracts from Apples on Polypyrrole as a Membrane for Phenol Removal, *Jurnal Kimia Sains dan Aplikasi*, 24, 2, pp. 62–69, <https://doi:10.14710/jksa.24.2.62-69>
4. Mulder. M, Basic Principles of Membrane Technology. Springer, (1996).
5. Nguyen. H. T. V, Ngo. T. H.A, Do. K. D, Nguyen. M. N, Dang. N.T.T, Nguyen. T.T.H, Vien. V, Vu.T. A. (2019). Preparation and Characterization of a Hydrophilic Polysulfone Membrane Using Graphene Oxide, *J Chem*, 2019, 1–10, <https://doi:10.1155/2019/3164373>
6. B. Hu, L. Miao, Y. Zhao, and C. Lü., (2017). Azide-assisted crosslinked quaternized polysulfone with reduced graphene oxide for highly stable anion exchange membranes, *J Membr Sci*, 530, 84–94, <https://doi:10.1016/j.memsci.2017.02.023>
7. R. A. Lusiana, N. A. Sasongko, V. D. A. Sangkota, N. B. A. Prasetya, P. Siahaan, A. A. Kiswandono, M. H. D. Othman., (2020). In-Vitro Study of Polysulfone-polyethylene glycol/chitosan (PEG-PSf/CS) Membranes for Urea and Creatinine Permeation, *Jurnal Kimia Sains dan Aplikasi*, 23, 8, 283–289, <https://doi:10.14710/jksa.23.8.283-289>
8. H. Junoh, J. Jaafar, N.A. H. Md. Nordin, A. F. Ismail, M. H. D. Othman, M. A. Rahman, F. Aziz, N. Yusof., (2020). Synthetic polymer-based membranes for direct methanol fuel cell (DMFC) applications, *Synthetic Polymeric Membranes for Advanced Water Treatment, Gas Separation, and Energy Sustainability*, Elsevier, 337–363. <https://doi:10.1016/B978-0-12-818485-1.00015-0>
9. R. A. Lusiana, R. Nuryanto, N. B. A. Prasetya, R. P. Sherina, and D. Dayanti., (2023). Eco-Friendly Chitosan-Based Biodiesel Heterogeneous Catalyst Support Membrane, *Jurnal Kimia Sains dan Aplikasi*, 26, 2, 39–49, <https://doi:10.14710/jksa.26.2.39-49>
10. A. Murniati, B. Buchari, S. Gandasasmita, Z. Nurachman, and N. Nurhanifah., (2018). Characterization of polyphenol oxidase application as phenol removal in extracts of rejected white oyster mushrooms (*pleurotus ostreatus*), *Oriental Journal of Chemistry*, 34, 3, 1457–1468, <http://dx.doi.org/10.13005/ojc/340336>
11. A. Murniati, N.A. Fajriana, G.A. Nugraha, R.M. Ibrahim, A Hardian, B. Buchari, S. Gandasasmita, Z. Nurachman., (2024). Textile Wastewater Treatment Using Polypyrrole / Polyphenol Oxidase Membranes,

- Jurnal Kimia Sains dan Aplikasi, 27, 2, 83–90, <https://doi.org/10.14710/jksa.27.2.83-90>
12. A. Murniati B. Buchari, S. Gandasasmita, Z. Nurachman, V.A. Kusumaningtyas, Jasmansyah, S. Budiman, A. Hardian, S. Herlinawati, R. M. Ibrahim., (2021). Modification of Cu<sup>2+</sup> in polyphenol oxidase extract from purple eggplant for phenol degradation in coal wastewater treatment, *IOP Conf Ser Earth Environ Sci*, 882, 1, 1-11, <https://doi:10.1088/1755-1315/882/1/012071>
  13. Y. Feng, G. Han, T. S. Chung, M. Weber, N. Widjojo, and C. Maletzko., (2017). Effects of polyethylene glycol on membrane formation and properties of hydrophilic sulfonated polyphenylenesulfone (sPPSU) membranes., *J Memb Sci*, 531, 27–35, <https://doi:10.1016/j.memsci.2017.02.040>
  14. S. Mulyati, F. Razi, and Zuhra., (2017). Characteristic of Polyethersulfone (PES) Asymmetric Membrane with Dimethyl Formamide and N-Methyl Pyrrolidone as Solvent, *Biopropal Industri*, 8, 55-62, <https://doi:10.36974/jbi.v8i1.1617>
  15. R. A. Lusiana and N. B. A. Prasetya., (2020). Pengaruh Penambahan Aditif terhadap Karakterisasi Fisikokimia Membran Polisulfon, *Indonesian Journal of Chemical Science*, 9,3, 194–200 <http://journal.unnes.ac.id/sju/index.php/ijcs>
  16. D. Alvianto, F. A. A. Nurhadi, A. W. Putranto, B. D. Argo, M. B. Hermanto, and Y. Wibisono., (2022). Sintesis dan Karakterisasi Membran Selulosa Asetat dengan Penambahan Antibiofouling Alami Ekstrak Bawang Putih, *Alchemy Jurnal Penelitian Kimia*, 18, 2,193–204 <http://doi:10.20961/alchemy.18.2.57199.193-204>
  17. A. Murniati, S.Shard, I. Fauzi, A. Hardian, R. M. Ibrahim, B. Buchari, S. Gandasasmita, Z. Nurachman., (2022). Immobilization of Crude Polyphenol Oxidase Purple Eggplant Extract on Chitosan membrane for Removal of Phenol Wastewater. *European Chemical Bulletin*,11,10 <http://doi:10.31838/ecb/2022.11.10.016>
  18. H. Yang, J. Zhou, Z. Wang, X. Shi, and Y. Wang., (2020). Selective swelling of polysulfone/poly(ethylene glycol) block copolymer towards fouling-resistant ultrafiltration membranes, *Chin J Chem Eng*, 28, 1, 98–103, <http://doi:10.1016/j.cjche.2019.03.011>
  19. S. Muljani, K. A. Kusuma, L. Nofitasari, A. R. Amalia, and N. Hapsari., (2018). Sintesis Membran Kitosan Silika Dari Geothermal Sludge, *Jurnal Teknik Kimia*, 13, 1, 22-26, <http://doi:10.33005/tekkim.v13i1.1150>
  20. S. Mulyati, S. Aprilia, Safiah, Syawaliah, M. A. Armando, and H. Mawardi., (2018). The effect of poly ethylene glycol additive on the characteristics and performance of cellulose acetate ultrafiltration membrane for removal of Cr (III) from aqueous solution, in *IOP Conference Series: Materials Science and Engineering*, Institute of Physics Publishing, 352, 1-7, <http://doi:10.1088/1757-899X/352/1/012051>
  21. I. Syahbanu, B. Piluharto, S. Khairi, and Sudarko., (2018). Effect of Evaporation Time on Separation Performance of Polysulfone/Cellulose Acetate (PSF/CA) Membrane, *IOP Conf Ser Mater Sci Eng*, 2991, 1-10, <http://doi:10.1088/1757-899X/2991/1/012040>
  22. R. O. Tasci, M. A. Kaya, and M. Celebi., (2022). Hydrophilicity and flux properties improvement of high performance polysulfone membranes via sulfonation and blending with Poly(lactic acid), *High Perform Polym*, 34, 10, 1115–1130, <http://doi:10.1177/09540083221110031>
  23. G. Mohd. Nawawi and L. T. N. Tram., (2012). Pervaporation Dehydration of Isopropanol–Water Mixtures Using Chitosan Zeolite–A Membranes, *J Teknol*, <http://doi:10.11113/jt.v41.719>
  24. D. Hermanto, M. Mudasir, D. Siswanta, and B. Kuswandi., (2019). Synthesis of Alginate-Chitosan Polyelectrolyte Complex (PEC) Membrane and Its Physical-Mechanical Properties, *Jurnal Kimia Sains*



25. Kayani. A, Raza. M. A, Raza. A, Hussain. T, Akram. M. S, Sabir. A, Islam. A, Haider. B, Khan. R.U, and Park. S.H. (2021). Effect Of Varying Amount Of Polyethylene Glycol (Peg-600) And 3-Aminopropyltriethoxysilane On The Properties Of Chitosan Based Reverse Osmosis Membranes, *International Journal of Molecular Sciences*. 22, 5, pp. 1–15, doi: 10.3390/ijms22052290.
26. J. Y. Park, M. H. Acar, A. Akthakul, W. Kuhlman, and A. M. Mayes., (2006). Polysulfone-graft-poly(ethylene glycol) graft copolymers for surface modification of polysulfone membranes, *Biomaterials*, 27, 6, 856–865, <https://doi.org/10.1016/j.biomaterials.2005.07.010>
27. Lusiana. R. A, Lusiana, Sasongko. N. A, Sangkota. V. D, Prasetya, Nor. B. A, A.et al., (2020) In-Vitro Study of Polysulfone-polyethylene glycol/chitosan (PEG-PSf/CS) Membranes for Urea and Creatinine Permeation, *Jurnal Kimia Sains dan Aplikasi*, 23, 8, pp. 283–289, <https://doi:10.14710/jksa.23.8.283-289>.
28. Akther. N, Daer. S, Hasan. S. W., 2018. Effect of flow rate, draw solution concentration and temperature on the performance of TFC FO membrane, and the potential use of ro reject brine as a draw solution in FO–RO hybrid systems, *Desalination Water Treat*, 136, pp. 65–71, <https://doi.org/10.5004/dwt.2018.23195>
29. Hakami. M. W, Alkhudhiri. A, Al-Batty. S, Zacharof. M. P, Maddy. J, and Hilal. N. 2020. Ceramic Microfiltration Membranes In Wastewater Treatment: Filtration Behavior, Fouling And Prevention, *Membranes*, 10, 9, pp 134. <https://10.3390/membranes10090248>

**How to cite this article:**

Aprillianti RN, Rahayu M, Hardian A, Murniati A. (2024). Effect of Polyethylene Glycol Concentration on the Structural and Mechanical Properties of Polysulfone-Based Membranes. *Journal of Chemistry and Environment*. 3(2). p. 25-38.